Supra-regional Brain Systems and the Neuropathology of Schizophrenia

I.C. Wright, T. Sharma, Z.R. Ellison, P.K. McGuire, K.J. Friston[1], M.J. Brammer, R.M. Murray and E.T. Bullmore

Department of Psychological Medicine, Institute of Psychiatry, King's College, London and [1]Wellcome Department of Cognitive Neurology, Institute of Neurology, University College, London, UK

At what levels of brain organization might pathological change in schizophrenia be anatomically expressed: global, regional or supra-regional? We hypothesised that brain structure reflects a set of supra-regional anatomical systems with common developmental influences. We conducted an exploratory analysis to identify supra-regional brain systems and to investigate whether abnormal brain architecture in schizophrenia is manifested within one or more of these systems. Magnetic resonance (MR) images were acquired from 27 patients with schizophrenia and 37 control subjects. After segmentation and registration of each individual MRI dataset in the standard space of Talairach and Tournoux, grey matter and ventricular-cerebrospinal fluid (CSF) maps were automatically parcellated into 104 regions. We used principal components analysis of the multiple regional grey matter and ventricular-CSF measurements, on all 64 subjects, to extract the five main normative supra-regional systems. The first two of these components represented global variation in grey matter and ventricular-CSF regional measures. We interpreted the other three components as representing supra-regional systems comprising: a frontal–parietal system, a frontal–temporal system and a frontal–basal ganglia system. Schizophrenic group mean scores on the first component (global grey matter–ventricular contrast) and fourth component (frontal–temporal system) were significantly reduced compared to controls. These results suggest that pathological change in schizophrenia may be expressed at two mutually independent levels of anatomical organization: global change in a grey matter/ventricular system and supra-regional change in a frontal–temporal system.

Introduction

Several studies, including two meta-analyses, have found changes in *global* brain measures in schizophrenia: reduced cerebral volume (Ward *et al.*, 1996), reduced cortical grey matter (Zipursky *et al.*, 1992; Harvey *et al.*, 1993; Lim *et al.*, 1996), and increased ventricle-to-brain ratio (Van Horn and McManus, 1992). Other groups have reported significant *regional* reductions of volume in several different 'regions of interest' (ROIs) studied (Lawrie and Abukmeil, 1998), including the hippocampus (Suddath *et al.*, 1990; Bogerts *et al.*, 1993; Nelson *et al.*, 1998), parahippocampal gyrus (DeLisi *et al.*, 1991; Shenton *et al.*, 1992; Kawasaki *et al.*, 1993), amygdala (Breier *et al.*, 1992; Kawasaki *et al.*, 1993), superior temporal gyrus (Barta *et al.*, 1990; Shenton *et al.*, 1992; Schlaepfer *et al.,* 1994; Flaum *et al.*, 1995), frontal cortex (Breier *et al.*, 1992; Kawasaki *et al.*, 1993; Andreasen *et al.*, 1994; Schlaepfer *et al.,* 1994; Buchanan *et al.*, 1998; Sullivan *et al.*, 1998) and thalamus (Andreasen *et al.*, 1994). If structural changes in schizophrenia are present in multiple brain regions, then can they be anatomically characterized by abnormality at a *supra-regional* level of brain organization?

Anatomical structures can generally be deconstructed into supra-regional systems by principal components analysis (PCA) of the covariances or correlations in size between their regional elements (Olson, 1958) (e.g. Joliffe, 1986; Vitt *et al.*, 1997). This mathematical operation has proved interesting in several previous biomorphometric applications because regional elements of supra-regional systems defined by PCA have often been found to share developmental influences or to have a common function (Cheverud, 1982).

A supra-regional analysis is particularly attractive for the investigation of brain changes in schizophrenia for two theoretical reasons. Firstly, there has been a recent renaissance of interest in the idea originally proposed by Wernicke (Wernicke, 1894), that psychotic disorder arises from pathological change in circuits or networks of anatomically interconnected brain regions (Friston and Frith, 1995; McGuire and Frith, 1996). Patterns of correlated change in regional cerebral blood flow (rCBF) measured by positron emission tomography (PET) have been analysed by multivariate statistical methods (Friston *et al.*, 1993) and there is evidence that patients with schizophrenia demonstrate abnormally correlated or 'functionally dysconnected' rCBF changes between left dorsolateral prefrontal cortex (DLPFC) and bilateral superior temporal gyri during performance of a word generation task (Friston *et al.*, 1994). There is also preliminary evidence from multivariate and correlational analyses of structural imaging data that temporal regional volumes may be abnormally correlated (Tien *et al.*, 1996) and that functional dysconnectivity in the prefrontal–temporal axis may be anatomically determined (Bullmore, 1998). Secondly, there is considerable evidence in support of neurodevelopmental models for the pathogenesis of schizophrenia (Murray and Lewis, 1987; Weinberger, 1987, 1996; Lane *et al.*, 1997). One study of structural brain changes in subjects at high risk of developing schizophrenia has suggested that the changes may result from at least two independent processes based on different combinations of genetic and perinatal influences (Cannon *et al.*, 1989). Since supra-regional systems in biomorphological structures often share common developmental influences (Cheverud, 1984), these systems may constitute the natural units for measuring subtle developmental abnormalities. In short, a supra-regional analysis of brain structure is relevant to both dysconnectionist and neurodevelopmental concepts of schizophrenia.

Here we report an analysis to investigate: (i) whether PCA applied to regional brain measures would extract components which could be interpreted meaningfully in terms of normal brain architecture and function; and (ii) whether there were quantitative differences between schizophrenia and control groups in their scores on these 'normative' components.

In order to determine the normative systems, we first segmented each individual MRI dataset into grey matter and ventricular-cerebrospinal fluid (CSF) maps in the standard space of Talairach and Tournoux (Talairach, 1988). These maps were then automatically parcellated into 104 regions. As our sample sizes were small compared to the number of regions, we

Table 1
Clinical and demographic characteristics of subjects

	Schizophrenic subjects	Controls
Number	27	37
Mean age in years (SD)	36 (11)	33 (12)
Gender	16 male; 11 female	19 male; 18 female
Handedness	25 right; 2 left	33 right; 4 left
Mean duration of illness in years	14	–

combined data from both groups (after removing between-group regional mean differences) for PCA (Atchley *et al.*, 1981).

Materials and Methods

Subjects

All subjects gave written informed consent to participate in the project which was approved by the local hospital ethical committee.

Thirty-four patients satisfying DSM-IV criteria for schizophrenia (American Psychiatric Association, 1994) were recruited from 16 families with two or more schizophrenic members. Thirty-nine unrelated healthy controls were also recruited. Characteristics of the sample are described in Table 1. The two groups were matched for age, sex and handedness. Images which did not fulfil quality control criteria (due to movement artefact, incomplete brain coverage or gross neuropathological abnormalities) were excluded. Images from 27 subjects with schizophrenia and 37 controls were suitable for analysis. The images described in this study have also contributed to other studies investigating brain structure in schizophrenia by multiple univariate analyses of the volumes of several brain regions (Frangou, 1997; Sharma *et al.*, 1998) and of grey matter density at each voxel (Wright *et al.*, 1999).

MRI Scanning

Acquisition Parameters

T_1-weighted spoiled-gradient recalled magnetic resonance images were acquired of the whole brain in the coronal plane with a 1.5 Tesla General Electrics Signa System (General Electrics, Milwaukee WI, USA): T_R 35 ms, T_E 5 ms, flip angle 35°, number of excitations = 1, field of view 20 cm, 256 × 256 matrix × 124 interleaved contiguous slices of 1.5 mm thickness.

Image Segmentation and Registration

Images were reoriented parallel to the intercommissural line, and segmented into binary maps of (i) grey matter and (ii) ventricular-CSF tissue classes, using methods described previously (Wright *et al.*, 1995, 1999). Thus for the grey matter maps, the grey matter in each scan was segmented: grey matter voxels were set to a uniform intensity value of 1 and voxels of other tissue classes were set to a value of 0, producing a binary grey matter image. These images were smoothed with a Gaussian filter (8 mm full-width half-maximum), which involves taking a local weighted average (with the weighting function having a Gaussian distribution) of the voxel values in the segmented MR scans. This step permits voxel-based statistical analysis of grey matter differences by assigning to each voxel a weighted sum of grey matter values under the volume of the smoothing filter employed. This weighted sum reflects the proportion of the volume of the kernel that has been labelled 'grey matter' and the term 'grey matter density' is used here with this specific meaning. These maps were then co-registered with a template image in the standard space of Talairach and Tournoux (Talairach, 1988) by affine and non-linear transformations (the deformations used in SPM change the spatial relations of the voxels but not their intensity values). All MR images were processed blind to subject identity and diagnosis, using ANALYZE (Robb, 1990) and Statistical Parametric Mapping (SPM) software (Friston *et al.*, 1995).

These steps resulted in a grey matter density map and a ventricular-CSF density map for each subject in standard space, i.e. each voxel in these maps was identified by a unique set of three-dimensional coordinates in the same stereotactic space. Due to spatial smoothing of the maps, each voxel value effectively represented the volume of grey matter within a locality (centred on each voxel) of a size corresponding to the width of the smoothing kernel, and voxel values in the transformed images are correlated with regional grey matter extent in the segmented untransformed images (Wright *et al.*, 1999). Similarly, voxel values within the ventricular map represented ventricular volumes in the locality of each voxel position.

Cerebral and Ventricular Parcellation

Grey and ventricular maps for each subject were automatically parcellated into 92 cerebral and 12 ventricular regions. The parcellation divided the cortex into regions corresponding approximately to Brodmann's areas, and divided subcortical grey matter into its main nuclei (e.g. thalamus) plus the cerebellum. The lateral ventricles were divided into their main components (frontal pole, central, trigone, occipital pole, posterior and anterior temporal horns).

This was done by first assigning one or more sets of index coordinates in the standard three-dimensional space of Talairach and Tournoux (Talairach, 1988) to each cerebral and ventricular region of interest, based on the consensus view of three of the authors (I.W., E.B., M.B.). The authors used the horizontal slices of the Talairach atlas to identify regions, supplemented by the coronal and sagittal slices of the Talairach atlas and other anatomical atlases and textbooks (Brodmann, 1909; Mesulam, 1985; Paxinos, 1990; Berry, 1995; Mai *et al.*, 1997). The Euclidean distances between a given voxel in the grey matter maps and the index coordinates for all (92) cerebral regions were computed, and that voxel was assigned to the region which had index coordinates separated by the smallest Euclidean distance (over all sets of index coordinates) from it in standard space. This minimum distance rule was likewise applied to assign each voxel in the ventricular CSF maps to one of the 12 possible regions of the lateral ventricles.

The sets of three-dimensional coordinates indexing each cerebral and ventricular region are given in Appendix 1; Figure 1 shows the result of parcellating grey matter and ventricular CSF maps by minimum Euclidean distance on the basis of this set of index coordinates.

After parcellation, regional mean grey matter densities were calculated for each subject by dividing the sum of grey matter densities within a region by the number of voxels it contained. Regional mean ventricular CSF densities were calculated in a similar fashion.

Multivariate Analysis

From these measurements, we constructed multivariate data matrices for the combined groups and the control and schizophrenic groups separately. We denote the ($n \times p$) data matrix for the combined groups $\mathbf{X_A}$ (n = 64), the data matrix for the control group $\mathbf{X_C}$ (n = 37) and the data matrix for the schizophrenic group $\mathbf{X_S}$ (n = 27). In each case, the number of variables p = 104, and each variable (or column) was scaled to have zero mean and unit variance.

We used singular value decomposition (SVD) to obtain the principal components of each of these matrices (Joliffe, 1986; Bullmore *et al.*, 1996). In general, the first principal component (PC) of a multivariate data matrix is that weighted sum of the variables which has the greatest variance of all possible weighted sums, subject to the constraint that the (eigen)vector of variable weights or loadings has unit length (this constraint also applies to subsequent PCs). The second PC is the weighted sum of the variables that has the largest variance of all possible weighted sums, subject to the constraint that it is orthogonal to (or uncorrelated with) the first PC; the third PC is the weighted sum of the variables that has the largest variance of all weighted sums subject to being orthogonal to the first and second PCs, and so on. In the context of this application, we can therefore think of the principal components as a set of mutually independent supra-regional anatomical systems or modes of (co)variation, ranked in order of their importance in accounting for the total variance–covariance of the data. The brain regions comprising, say, the second system can be identified as those variables which have a large loading on the second eigenvector; the importance of this system in accounting for total variance–covariance can be assessed by inspection of the second eigenvalue; and the salience with which the system is expressed in an individual image, or group of images, can be quantified by the second PC score(s) for that individual or group.

Extraction of eigenvectors, eigenvalues and PC scores is illustrated by

Table 2
Principal components of combined, schizophrenia and control group data matrices

Principal component	Combined matrix		Schizophrenia group matrix		Control group matrix	
	Eigenvalue (Λ)	% cumulative variance	Eigenvalue (Λ)	% cumulative variance	Eigenvalue (Λ)	% cumulative variance
PC1	7.3	52	7.6	55	7.2	49
PC2	2.9	60	3.0	64	3.1	59
PC3	2.4	66	2.5	70	2.7	66
PC4	2.0	70	2.3	75	2.2	70
PC5	1.9	73	1.9	78	2.1	74
PC6	1.8	76	1.7	81	2.0	78
PC7	1.5	79	1.6	84	1.6	81
PC8	1.4	80	1.5	86	1.5	83
PC9	1.3	82	1.4	88	1.5	85
PC10	1.2	83	1.3	89	1.3	87

considering the singular value decomposition of one of the data matrices, $\mathbf{X}$ which can be written:

$$\mathbf{X} = \mathbf{U}\Lambda\mathbf{V}^{T} \quad (1)$$

where $\mathbf{U}$ ($n \times r$) is an orthogonal matrix, Λ ($r \times r$) is a diagonal matrix, $\mathbf{V}$ ($p \times r$) is an orthogonal matrix, $\mathbf{V}^{T}$ represents the matrix transpose of $\mathbf{V}$, and $r = \min(n,p) = n$. We write the variance–covariance matrix of $\mathbf{X}$ as $\mathbf{X}^{T}\mathbf{X}$ and note that $\mathbf{X}^{T}\mathbf{X} = \mathbf{V}\Lambda^{2}\mathbf{V}^{T}$. It follows that the PC loadings or eigenvectors of $\mathbf{X}^{T}\mathbf{X}$ are given by the columns of $\mathbf{V}$; the PC variances or eigenvalues of $\mathbf{X}^{T}\mathbf{X}$ are given by the main diagonal elements of Λ^{2} and the standardized PC scores are given by $\mathbf{XV}$.

Extracting Normative Systems

One simple approach to deriving the normative principal components would be to use the principal components from the control group data matrix alone. However, the results of such an analysis might be unstable because the number of subjects is small relative to the number of variables. Therefore we chose to combine the groups in order to extract normative principal components (Atchley *et al.*, 1981). Assuming that the main components of variation were similar in the two groups, after removing between-group differences in regional mean values, we regressed the columns of $\mathbf{X}_{A}$ (the combined group data matrix) on a factor coding for group membership, and substituted each column by the residuals of this regression to generate a new data matrix $\mathbf{X}_{R}$ that was corrected for between-group differences in regional mean grey matter or CSF measures. Singular value decomposition of $\mathbf{X}_{R}$ yields an eigenvector matrix $\mathbf{V}_{R}$, the columns of which are a set of eigenvectors reflecting *within-group* variation. The first five eigenvectors, which accounted for 73% of the variance, were selected for further analysis (Table 2). The data matrix $\mathbf{X}_{A}$ was projected into the space of the first five eigenvectors of $\mathbf{V}_{R}$ to estimate the scores for each subject on each of these common principal components: $\mathbf{S}$ ($n \times 5$) = $\mathbf{X}_{A}\mathbf{V}_{R}$ (Atchley *et al.*, 1981).

Supra-regional Hypothesis Testing

We wished to test the null hypothesis that there was no quantitative difference *between* groups in their PC scores for this set of normative principal components. As some of the 27 subjects in the schizophrenia group were siblings from the same 16 families, we considered the possibility that the scores for siblings would be correlated and therefore that it would be inappropriate to use a two-sample *t*-test (which assumes independence of scores within the group). Instead, we fitted a mixed effects model, in STATA 5.0, to estimate the effect of group membership (schizophrenia versus control) on each PC score, with family membership modelled as a random effect. For each PC, we modelled the score $s_{i,t}$, from individual t and family i, as:

$$s_{i,t} = \beta_{0} + \beta_{1}x_{i,t} + u_{i} + \varepsilon_{i,t} \quad (2)$$

where β_{0} is a constant, $x_{i,t}$ is a dummy variable representing subject group, β_{1} is the group effect coefficient (to be estimated and tested against the standard normal distribution), u_{i} is the random family effect, and $\varepsilon_{i,t}$ an error term. A two-tailed *P*-value <0.05 was considered significant. We did not correct the significance level for these *P*-values with a Bonferroni adjustment (Perneger, 1998) since we were interested in whether there was a difference between the groups on each of the five principal components.

We also tested our assumption (used in deriving the normative principal components) that the first five supra-regional systems were qualitatively similar in the schizophrenic and control groups, i.e. that the same regions were loaded to approximately the same degree on the first five principal components separately extracted from each group.

More geometrically, this involved testing the null hypothesis that the k-dimensional subspace defined by the first k eigenvectors of the control group data (first k columns of $\mathbf{V}_{C}$) in the p-dimensional space of the original variables was not clearly separated from the k-dimensional subspace defined by the first k eigenvectors of the schizophrenic group data (first k columns of $\mathbf{V}_{S}$) (Krzanowski, 1988). The minimum angle between any control group eigenvector and the schizophrenic group eigenvector most nearly parallel to it is given by:

$$\alpha = \cos^{-1}\sqrt{\Lambda_{1}} \quad (3)$$

where Λ_{1} is the largest eigenvalue of $\mathbf{N}$, and $\mathbf{N}$ ($p \times p$) is defined by:

$$\Lambda_{1} = \mathbf{V}_{C}\mathbf{V}_{S}^{T}\mathbf{V}_{S}\mathbf{V}_{C}^{T} \quad (4)$$

where $\mathbf{V}_{C}$ and $\mathbf{V}_{S}$ are both ($k \times p$) matrices comprising the first k eigenvectors of the controls and schizophrenic groups respectively. This minimum angle α between the k-dimensional subspaces defined by two sets of k eigenvectors has been described as a suitable measure for quantifying the extent to which the two subspaces coincide (Krzanowski, 1979). The smaller the size of α, the more likely it is that the two subspaces (sets of eigenvectors) are the same, and therefore the less likely it is that there are qualitative group differences in supra-regional anatomy.

To test the probability of the observed minimum angle $\alpha = \cos^{-1}\sqrt{\Lambda_{1}}$ under the null hypothesis of zero between-group difference, we adopted a bootstrap procedure. The subjects were randomly resampled with replacement to create two bootstrapped groups of the same sizes (27 and 37 individuals) as the original groups. The eigenvector matrices were obtained by SVD for each bootstrapped group, and the minimum angle between eigenvector matrices was computed. This procedure was repeated 1000 times to generate a bootstrap distribution of α (Efron, 1993). The probability P that an angle as large as the observed angle could have occurred by chance was estimated by the number of entries in the bootstrap distribution which exceeded the observed angle divided by the total number of bootstrap estimates of α (1000). A *P*-value <0.05 was considered significant.

Stability of Eigenvectors

Despite combining mean-corrected data from both groups to extract PCs, the total number of subjects is smaller than the number of variables, which might render the results of the singular value decomposition unstable. Therefore, we examined the stability of the first five eigenvectors using two indices. Firstly, we estimated confidence cones for the eigenvectors of $\mathbf{X}_{R}$ using the method of Beran and Srivastava (Beran and Srivastava, 1985). If the eigenvector is imagined to be a vector of unit length extending from the origin, then the confidence cone surrounds it in multidimensional space: the narrower the cone, the greater the stability of its coefficients. For each eigenvector, k ($k = 1, \ldots, 5$), we calculated the function:

$$c_{k} = |\mathbf{V'}_{A,k}^{T}\,\mathbf{V}_{A,k}| \quad (5)$$

We generated a bootstrap distribution for c_{k} from 200 bootstrap replications of $\mathbf{X}_{A}$ by random resampling (with replacement) of the rows of $\mathbf{X}_{A}$ followed by SVD to obtain $\mathbf{V'}_{A}$ [for details, see Beran and Srivastava (Beran and Srivastava, 1985)]. The 75% confidence cone index d_{k} was obtained from the lower 25% point of the bootstrap distribution for c_{k}. This index ranges between 0 (wide confidence cone) and 1 (narrow confidence cone). Secondly, as our interpretations of the eigenvectors

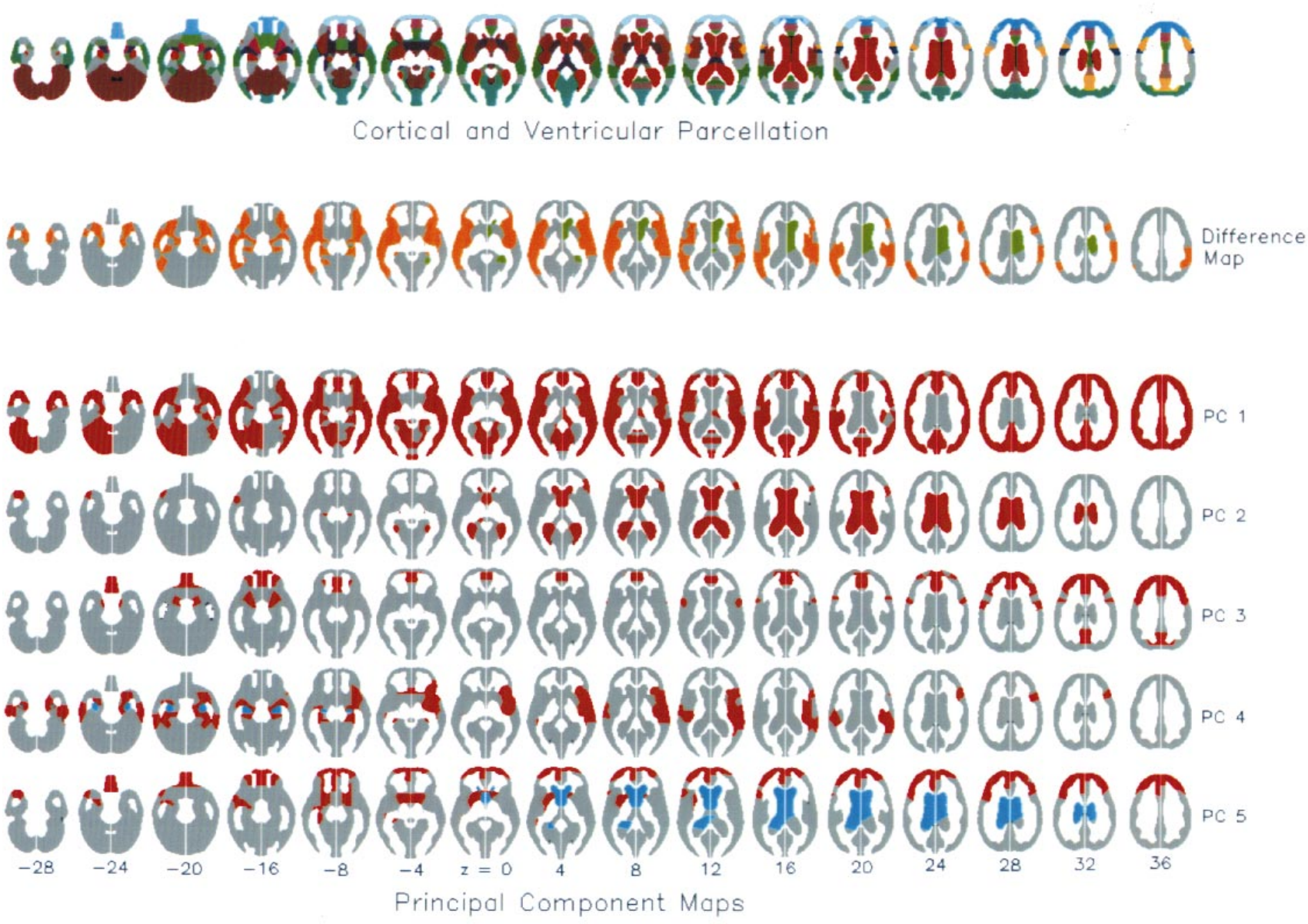

Figure 1. Maps in Talairach space at axial levels from $z = -28$ mm to $z = +36$ mm. The left side of each slice represents the right hemisphere. (Upper) Template image showing cortical and ventricular parcellation. (Middle) Difference map of regional grey matter and ventricular-CSF differences between schizophrenia and control groups. A *t*-test for the differences in group means was performed for each region and the results were rescaled to display regions with highest means in the control group (orange) and highest means in the schizophrenia group (green). (Lower) Five sets of images showing all cerebral and ventricular regions with eigenvector loadings >0.1 (in red) and ventricular-CSF regions with eigenvector loadings <–0.1 (in blue) for the five major PCs of the combined schizophrenia and control groups. For clarity, cerebral regions with loadings <–0.1 are not displayed in a separate colour.

Table 3
Differences in principal component scores between schizophrenia (SZ) and control (CO) groups

Principal component	SZ		CO		Group coefficient β_1	Standard error β_1	z score	*p*
	Mean	SD	Mean	SD				
PC1: global grey matter–global ventricular contrast	–2.7	7.9	2.0	6.7	–4.7	1.8	–2.63	0.01
PC2: global ventricular system	0.4	2.9	–0.3	2.9	0.7	0.7	0.98	0.33
PC3: frontal–parietal system	–0.02	2.2	0.01	2.6	–0.1	0.6	–0.07	0.95
PC4: frontal–temporal system	–0.66	2.3	0.48	1.9	–1.1	0.5	–2.20	0.03
PC5: frontal–basal ganglia system	–0.07	1.7	0.05	1.9	–0.2	0.5	–0.31	0.76

were based on considering regions with coefficients of absolute magnitude greater than 0.1 important, we calculated a similarity coefficient (κ) for the first five eigenvectors of $\mathbf{X}_A$, again using the 200 bootstrap replications of $\mathbf{X}_A$. We used the total number of regions where the eigenvector coefficient was of absolute magnitude >0.1 in both $\mathbf{V}'_{A,k}$ and $\mathbf{V}_{A,k}$ (= *a*), or >0.1 in one vector but <0.1 in the other (= *b*). From these we calculated the Czekanowski dissimilarity coefficient [*b*/(2*a* + *b*)] (Krzanowski, 1988) and defined the similarity coefficient as:

$$\kappa = 1 - b/(2a + b) \quad (6)$$

This coefficient decreases from 1 (identical matching in all bootstrap replications) towards zero as the matching of regions with absolute coefficient values greater than 0.1 declines.

Results

Normative Supra-regional Brain Systems

The first ten eigenvalues obtained by SVD of $\mathbf{X}_R$ are given in Table 2. The loadings of all 104 regional variables on the first five eigenvectors are given in Appendix 2, with the values for the eigenvector 75% confidence cones (d_k) and similarity coefficients (κ). The sign of each eigenvector is arbitrary (i.e. the vector coefficients can be multiplied by –1). Cerebral and ventricular regions with eigenvector loadings of >0.1 and ventricular regions with loadings <–0.1 are displayed in Figure 1 (for clarity, cerebral regions with loadings <–0.1 are not displayed separately).

The first PC had positive eigenvector loadings for grey matter regions and small negative loadings for ventricular regions. Therefore it represented a global grey matter/ventricular contrast.

The second PC had large *positive* eigenvector loadings for ventricular regions (>0.2 for all regions except the temporal horns) and relatively small loadings on grey matter regions. Therefore, this component largely represented a global ventricular system (or at least the component of global ventricular variance not orthogonally accounted for by the first PC).

The third PC had *positive* eigenvector loadings (>0.1) for bilateral premotor, prefrontal, superior parietal lobule and precuneus grey matter regions. The *negative* loadings (<–0.1) were for subcortical and retrosplenial structures. Brain regions positively loading on this component can be considered to represent a frontal–parietal system.

The fourth PC had *positive* eigenvector loadings (>0.1) for left inferior frontal grey matter, temporal grey matter regions (bilateral hippocampus, parahippocampus, inferior temporal gyrus, primary auditory cortex, auditory association cortex and left superior temporal gyrus) and left insula grey matter. The *negative* loadings included occipital, subcallosal and frontal pole grey matter and the bilateral anterior temporal horns of the ventricles. Brain regions positively loading on this eigenvector can be considered to represent a frontal–temporal system.

The fifth PC had *positive* eigenvector loadings (>0.1) for frontal regional grey matter (including DLPFC, frontal pole and orbitofrontal cortex) and the basal ganglia (bilateral putamen and corpus striatum). The *negative* loadings included occipital and temporal regional grey matter, and the bilateral frontal horns and central regions of the ventricles. Brain regions positively loading on this eigenvector can be considered to represent a frontal–basal ganglia system.

Between the first and the fifth PC, the 75% confidence cone index (d_k) declined from 0.99 to 0.28 and the similarity coefficient κ from 0.92 to 0.47. This indicates that the eigenvector coefficients become more unstable for PCs 3–5 and thus our interpretations for these PCs must be more tentative.

Differences in Normative Supra-regional Anatomy Between Groups

There were significant differences between the two groups in their scores on the first and fourth PCs (Table 3). The schizophrenics had lower scores on the first PC ($P = 0.01$), i.e. they had globally reduced grey matter and globally increased ventricular-CSF measures. Schizophrenics also had lower scores on the fourth PC ($P = 0.03$), i.e. they had reduced grey matter measures in a supra-regional system comprising left prefrontal, temporal (lateral and medial) and insular grey matter (after taking into account grey matter changes in orthogonal systems). Overall differences in regional grey matter and ventricular-CSF between the two groups are illustrated in Figure 1.

Within-group Supra-regional Anatomy

The first ten eigenvalues Λ_i, $i = 1, \ldots, 10$, obtained separately for each group by SVD of the data matrices $\mathbf{X}_C$ and $\mathbf{X}_S$, are given in Table 2. It can be seen that the two groups have very similar eigenvalue profiles. In both groups, the first five eigenvalues accounted for a large majority of the total variance: 78% of the variance in the schizophrenic group and 74% of the variance in the control group.

The minimum angle between the two five-dimensional subspaces defined by the first five columns of $\mathbf{V}_C$ and $\mathbf{V}_S$ was 9.0°. The probability of a minimum angle as large as this arising under the null hypothesis was estimated by bootstrap as $P = 0.08$, i.e. greater than our threshold for significance. We concluded that at this level of significance there was no clear evidence for a qualitative difference in the first five supra-regional brain systems between the two groups.

Discussion

Normative Supra-regional Brain Systems

We have used singular value decomposition of multiple regional

measurements on MRI data from 64 subjects (37 schizophrenic patients and 27 control subjects) to identify five principal components that collectively accounted for >70% of total variance–covariance in the data.

Since PCA is an uninfomed multivariate procedure, its utility depends on whether meaningful biological interpretations can be ascribed to the different components. In biomorphometric applications, the first PC is often an index of global 'size' while the remaining PCs reflect different aspects of 'shape', although since our methods did not measure the exact volume of regions, this provides only an analogy for the interpretation of our results.

The morphological system associated with the largest proportion of total variance was a global grey matter/ventricular contrast. The existence of this system suggests that, at least after registration of imaging data in standard space, global grey matter and ventricular CSF densities are negatively correlated: the greater the global grey matter density, the smaller the global CSF density.

The second PC, a global ventricular system, represented variation in the lateral ventricular system which was orthogonal to ventricular CSF variance in the first principal component. This suggests that in addition to the component of ventricular variance inversely determined by variance in grey matter volume, there is another major component of ventricular variance that is independent of total grey matter volume.

The third, fourth and fifth PCs are more interesting from a supra-regional perspective. Brain regions positively loading on the third eigenvector included grey matter in bilateral frontal cortex, superior parietal lobule and precuneus. Frontal and parietal brain regions are known to be densely and reciprocally connected (Goldman-Rakic, 1988). This raises the possibility that this supra-regional system might represent the adult outcome of positively correlated growth in distributed brain regions that have enjoyed the mutually trophic effects of reciprocal afferentation since an early stage in development. In other words, the system may share a common developmental influence mediated by its anatomical inter-connectivity (Van Essen, 1997). Regional elements of the system might plausibly also function co-operatively in visuo-spatial processing and working memory, which have been shown to depend on integrated activation of frontal–parietal networks (Mellers *et al.*, 1995; Moscovitch *et al.*, 1995; Coull *et al.*, 1996; Salmon *et al.*, 1996; McCarthy *et al.*, 1997).

Brain regions positively loading on the fourth PC comprised a frontal–temporal system, including grey matter in left superior and bilateral inferior temporal gyri, hippocampus and parahippocampal gyrus bilaterally, and left inferior frontal gyrus. There is anatomical evidence from primate studies that these regions are also interconnected by axonal tracts (Petrides and Pandya, 1988). It has been proposed that there is a cortical association pathway for the auditory system running from primary auditory cortex, via auditory association areas, superior temporal gyrus and insula to the parahippocampus (Pandya and Yeterian, 1985). Thus, as in the case of the third PC, it may be that the existence of this system in the adult brain reflects mutually correlated growth determined by anatomical interconnectivity. This system also can plausibly be assigned common functions of auditory and linguistic processing.

Finally, brain regions positively loading on the fifth PC included grey matter in frontal cortical regions and the basal ganglia bilaterally. A major efferent connection of prefrontal cortex is to basal ganglia (Alexander *et al.*, 1990). This system may mediate a common function in prefrontal output processing, and might again be determined developmentally by the mutually trophic effects of early anatomical connectivity.

If two brain regions load on the same PC, then does this imply some degree of anatomical connectivity during development? Theoretically, three broad processes operating during development may lead to a correlation in size of two anatomically separate regions: (i) mutually trophic neural connections between the regions, (ii) similarities in gene expression, or (iii) similar responses to neuro-hormonal factors. We have consistently interpreted correlations between adult regional volumes in terms of anatomical connections between regions established in early life. In favour of this interpretation, it is known that neurotransmitters such as glutamate have trophic effects in the developing brain (Kerwin, 1993; Ben-Ari *et al.*, 1997). There is also evidence from animal studies that early focal brain lesions can lead to widespread cortical and subcortical maldevelopment (Kolb *et al.*, 1983, 1998), presumably via disturbances in anatomical connectivity. However, advances in understanding of the role of genetic and neuro-hormonal processes in controlling cortical patterning may clarify their contribution to anatomical correlations in the adult brain (Ross and Pearlson, 1996; Weickert and Weinberger, 1998).

Neuropathology of Schizophrenia

Two supra-regional systems were expressed differently in the schizophrenic group compared to controls. Schizophrenic group mean scores on the first PC (global grey matter/CSF contrast) and fourth PC (frontal–temporal system) were significantly reduced relative to controls (see Table 3). These results are broadly concordant with the body of evidence from both structural imaging and neuropathological studies of schizophrenia (see below). However, by adopting a multivariate approach, our analysis has provided several further insights into brain architectural abnormalities in schizophrenia. Firstly, global ventricular CSF and grey matter changes in schizophrenia are related (both loading on PC1). Secondly, frontal and temporal lobe changes are related (both loading on PC4). Finally, as the variance components associated with these PCs are, by definition, orthogonal, this suggests that at least two processes of structural change are involved.

The schizophrenics had a lower score for the global grey matter/ventricular contrast than the controls, indicating that they had relatively larger ventricles and relatively less global grey matter. The ventricular enlargement is consistent with the previous studies showing both increased ventricle-to-brain ratio in schizophrenics (Van Horn and McManus, 1992) and increased ventricular volume (Degreef *et al.*, 1992). The reduced global grey matter is consistent with imaging studies reporting reduced cortical grey matter in schizophrenia (Zipursky *et al.*, 1992, 1998; Lim *et al.*, 1996), and neuropathological studies reporting distributed grey matter changes associated with reduced cortical thickness and increased neuronal density (Selemon *et al.*, 1995, 1998). Our results indicate that these two changes are interdependent. Ventricular enlargement, which is considerable in structural images (mean lateral ventricular volume enlargement of 25%), may therefore be a sensitive marker for the more subtle loss of cortical grey matter.

The schizophrenics had a lower score for the frontal–temporal system than the controls, indicating that in this system they had relatively reduced grey matter within a bilateral temporal–left frontal brain system (associated with relatively larger temporal horns), after taking into account changes in orthogonal systems. Since the system represents a variance component, this result

does not necessarily imply absolute grey matter reductions in these regions. However, many of the individual regions comprising this system have previously been reported to have reduced volume in schizophrenic samples, including the left superior temporal gyrus (Barta *et al.*, 1990; Shenton *et al.*, 1992; Flaum *et al.*, 1995), bilateral hippocampus (Suddath *et al.*, 1990; Nelson *et al.*, 1998), bilateral parahippocampus (DeLisi *et al.*, 1991; Kawasaki *et al.*, 1993; Shenton *et al.*, 1992) and inferior prefrontal region (Buchanan *et al.*, 1998). Structural studies have also indicated that patients with schizophrenia may have cortical changes which preferentially affect frontal–temporal regions (Schlaepfer *et al.*, 1994, Sullivan *et al.*, 1998). Pathological studies have identified a variety of cellular and neurochemical abnormalities in both prefrontal cortex (Akbarian *et al.*, 1993, 1996; Selemon *et al.*, 1995, 1998; Daviss and Lewis, 1995; Akil and Lewis, 1996; Glantz and Lewis, 1997; Rajkowska *et al.*, 1998; Woo *et al.*, 1998) and temporal/limbic structures (Kovelman and Scheibel, 1984; Falkai and Bogerts, 1986; Jeste and Lohr, 1989; Akbarian *et al.*, 1993; Benes *et al.*, 1996, Young *et al.*, 1998) in schizophrenia. Functional imaging studies have identified abnormal prefrontal function in schizophrenia (Berman *et al.*, 1992; Weinberger *et al.*, 1992; Andreasen *et al.*, 1997; Curtis *et al.*, 1998) and have implicated both left prefrontal cortex (McGuire *et al.*, 1993) and the superior temporal cortex (Suzuki *et al.*, 1993; Woodruff *et al.*, 1995, 1997) in the pathophysiology of auditory hallucinations. Functional changes in prefrontal cortex have been related to structural changes in the medial temporal lobe (Weinberger *et al.*, 1992). Neurochemical changes in both prefrontal cortex and the hippocampi have been identified *in vivo* using proton magnetic resonance spectroscopy (Bertolino *et al.*, 1998). The anatomy of the fourth PC also appears similar to the left frontal–bitemporal system involved in verbal fluency, which has been found to show evidence of 'functional disconnection' in PET studies of schizophrenia (Friston *et al.*, 1994). Our results provide further support for theories which postulate that the pathology of schizophrenia involves abnormalities in a distributed frontal–temporal neural system (Weinberger *et al.*, 1992; Friston and Frith, 1995). The results of several pathological studies are consistent with underlying neural dysconnectivity within prefrontal and medial temporal regions (Selemon *et al.*, 1995; Glantz and Lewis, 1997; Young *et al.*, 1998). Primate studies indicate that neonatal lesions in the medial temporal lobe are associated with disturbances in adult prefrontal neurochemistry (Bertolino *et al.*, 1997), providing a possible pathophysiological mechanism for abnormality in this system. Finally, these lesions have been found to affect amphetamine-induced subcortical dopamine release (Saunders *et al.*, 1998), which has been demonstrated to be abnormal in patients with schizophrenia (Abi-Dargham *et al.*, 1998).

If two morphological systems are abnormal in familial schizophrenia, then what are the pathological mechanisms? Cannon *et al.* (Cannon *et al.*, 1989) suggested that that there were two types of structural deficit in schizophrenia: multi-site neural developmental deficit (reflecting cortical and cerebellar structural change) and periventricular damage (reflecting ventricular enlargement). The multi-site neural developmental deficit was associated with genetic risk for schizophrenia, while periventricular damage was associated with both genetic risk and a history of obstetric complications and low birth weight. This implied that the two types of structural change resulted from two rather different aetiological mechanisms. An alternative possibility is that a single genetic mechanism may influence two structural developmental pathways. Genetic pleiotropy implies that some genes have multiple effects and there are many examples of single gene disorders with developmental effects in multiple organ systems. Cheverud (Cheverud, 1982) analysed both phenotypic and genotypic correlation matrices for macaque cranium morphology and found evidence for genetic effects influencing several morphological systems.

Methodological Issues

For the investigation of the neuropathology of schizophrenia, our analysis has a number of potential advantages over studies employing univariate analyses of brain measures. Firstly, we carried out a comprehensive assessment of regional brain changes in schizophrenia by cerebral parcellation of segmented grey matter maps registered in standard space. In this way, we examined the major Brodmann areas of the cortex as well as the main subcortical structures. Secondly, the application of similar methods to the lateral ventricular system enabled us to integrate the very well established findings of ventricular change in schizophrenia with the apparently more subtle cortical/subcortical changes. Thirdly, by conducting a multivariate analysis using orthogonal PCs we have avoided the multiple comparisons problem which an equally comprehensive univariate analysis would entail. Fourthly, our analysis has addressed the existence of structural dependencies between brain regions which has allowed the interpretation of pathological changes within the context of interdependent systems (Goldman-Rakic and Selemon, 1997; Lewis, 1997). The potential of such an approach is well illustrated by the field of craniofacial disorders, in which supra-regional models have provided a framework for integrating diverse findings from morphological, developmental and genetic research (Harris and Smith, 1982; Saksena and Bixler, 1990; Bookstein, 1991; Dempsey *et al.*, 1995; Johnston and Bronsky, 1995; Mossey *et al.*, 1997; Seow *et al.*, 1998). It is of interest that craniofacial abnormalities have been identified in schizophrenia (Lane *et al.*, 1997). In the future, multivariate analyses may improve the discrimination of brain structure in patients with schizophrenia compared with control subjects, leading to improved diagnosis (Csernansky *et al.*, 1998).

Several limitations of the present study should be noted. First, we used an automatic technique for cerebral parcellation. Although this was highly reliable, its validity depends in part on the agreement of our technique with other methods of assigning Brodmann regions. We have based our assignment on the Talairach atlas, which is widely used internationally in structural and functional imaging studies. One of the problems with a standard atlas is that there is interindividual variability in the anatomical boundaries of Brodmann regions (Rajkowska and Goldman-Rakic, 1995). The biological validity of the technique also depends on the suitability of the Brodmann cytoarchitectonic map for cerebral parcellation. In view of the possible convergence we have noted between supra-regional organization of cortical elements and their anatomical interconnections, it might make sense in future to parcellate the cortex on the basis of myeloarchitectonic rather than cytoarchitectonic features.

Second, the grey matter and ventricular-CSF maps were derived from the segmentation of SPGR MR images. Techniques used for the segmentation of these images are less valid and reliable than for dual-echo MR images (Bullmore *et al.*, 1995). Artefactual variation introduced during segmentation may have inflated the variance associated with global grey matter or global

ventricular-CSF measures (and hence the value of the first eigenvalue).

Third, our sample size is not very large [although it is larger than another multivariate comparison (Csernansky *et al.*, 1998) of schizophrenia and control groups], and we have examined a large number of brain regions. Although this avoids arbitrary selection of a few regions of interest and may give a more complete picture of supra-regional brain organization, the results of our PCAs may be somewhat unstable, and need to be tested in further studies. In particular, the eigenvector confidence cones and similarity coefficients indicate that the stability of the PC coefficients decreases from the first to the fifth PC. There is also a risk, in the light of our sample size, that some of the negative results we have reported may be type 2 errors. In particular, we found no qualitative difference in supra-regional organization based on comparison of the two sets of eigenvectors from the control and schizophrenia groups considered separately. However, the probability under the null hypothesis of the observed difference was small (P = 0.08) and a previous study has found evidence of a comparable difference between (larger) control and schizophrenic samples in factor structure of multiple ROI measurements (Tien *et al.*, 1996). In principle, it would not be surprising if quantitative change in supra-regional organization was accompanied by qualitative change.

Fourth, although we have suggested that the results of the singular value decomposition may be interpreted in a way that is anatomically and functionally sensible, SVD is uninformed by any prior knowledge about organization of the nervous system. In future studies it would be interesting to test our interpretations using other multivariate methods, such as path analysis [see McIntosh (McIntosh, 1994), for an example from functional imaging] or comparison of covariance matrices (see Lofsvold, (Lofsvold, 1986) and Paulsen (Paulsen, 1994), for examples from genetics/biomorphometrics], which might be able to account for the observed correlations between multiple brain regions measured from adult imaging data in terms of pre-existing theories of brain organization (Young, 1993), development (Van Essen, 1997) or function.

Finally, our sample of patients with schizophrenia was recruited from families with two or more schizophrenic members. Therefore, our results may not generalize to other patients with sporadic schizophrenia, although one advantage in selecting patients with 'familial' schizophrenia in that it leads to a more homogeneous sample than schizophrenia in general. In addition, inclusion of siblings may have led to some correlation between brain measures of related subjects, leading to an effective reduction in the number of independent measures in the schizophrenia group. However, we have used random effects modelling to correct our tests of between-group differences for familial effects. This is an established statistical technique for dealing with 'litter effects' (Lange and Ryan, 1989) and modelling family membership as a random effect produced minimal changes in our results.

Conclusion

This is the first study, to our knowledge, which applies multivariate analysis to brain structure after comprehensive parcellation in this manner. By this approach we have overcome important limitations of 'region of interest' studies [as discussed by Tien *et al.* (Tien *et al.*, 1996)].

The results of this analysis, using exploratory statistics, suggest that brain structure may be represented by a number of supra-regional systems, developmentally determined by anatomical connectivity between cortical regions and subserving specific functions. Furthermore, pathological change in schizophrenia may be expressed at two mutually independent levels of anatomical organisation: global change in grey matter/ventricular system and supra-regional change in a frontal–temporal system. Although concepts such as frontal–temporal connectivity have been extensively discussed in the schizophrenia literature, there is a critical lack of structural studies providing anatomical evidence for or against these theories. Multivariate analysis of the parcellated brain provides a technique for investigating these theories as well as a basis for interpreting the spatial characteristics of relatively diffuse cortical changes.

Notes

The authors thank Dr S. Rabe-Hesketh and Dr P. Sham for statistical advice and four anonymous reviewers for their comments. I.C.W., K.J.F. and E.T.B. were supported by the Wellcome Trust. This work was also supported by the UK Medical Research Council (grant G9418453N) and by the Stanley Foundation (R.M.M.).

Address correspondence to Dr Ian Wright, Department of Psychological Medicine, Institute of Psychiatry, DeCrespigny Park, Denmark Hill, London SE5 8AF, UK. Email: spjuicw@iop.kcl.ac.uk.

References

Abi-Dargham A, Gil R, Krystal J, Baldwin RM, Seibyl JP, Bowers M, van Dyck CH, Charney DS, Innis RB, Laruelle M (1998) Increased striatal dopamine transmission in schizophrenia: confirmation in a second cohort. Am J Psychiat 155:761–767.

Akbarian S, Bunney WE, Jr, Potkin SG, Wigal SB, Hagman JO, Sandman CA, Jones EG (1993a) Altered distribution of nicotinamide-adenine dinucleotide phosphate-diaphorase cells in frontal lobe of schizophrenics implies disturbances of cortical development. Arch Gen Psychiat 50:169–177.

Akbarian S, Vinuela A, Kim JJ, Potkin SG, Bunney WE, Jr., Jones EG (1993b) Distorted distribution of nicotinamide-adenine dinucleotide phosphate-diaphorase neurons in temporal lobe of schizophrenics implies anomalous cortical development. Arch Gen Psychiat 50: 178–187.

Akbarian S, Sucher NJ, Bradley D, Tafazzoli A, Trinh D, Hetrick WP, Potkin SG, Sandman CA, Bunney WE, Jr, Jones EG (1996) Selective alterations in gene expression for NMDA receptor subunits in prefrontal cortex of schizophrenics. J Neurosci 16:19–30.

Akil M and Lewis DA (1996) Reduced dopamine innervation of the prefrontal cortex in schizophrenia. Soc Neurosci Abstr 22:1679.

Alexander GE, Crutcher MD, DeLong MR (1990) Basal ganglia-thalamocortical circuits: parallel substrates for motor, oculomotor, 'prefrontal' and 'limbic' functions. Prog Brain Res 85:119–146.

American Psychiatric Association (1994) Diagnostic and statistical manual of mental disorders (DSM-IV), 4th edn. Washington, DC: American Psychiatric Association.

Andreasen NC, Arndt S, Swayze V, II, Cizadlo T, Flaum M, D OL, Ehrhardt JC, Yuh WT (1994) Thalamic abnormalities in schizophrenia visualized through magnetic resonance image averaging. Science 266:294–298.

Andreasen NC, Flashman L, Flaum M, Arndt S, Swayze V, II, DS OL, Ehrhardt JC, Yuh WT (1994) Regional brain abnormalities in schizophrenia measured with magnetic resonance imaging. J Am Med Assoc 272:1763–1769.

Andreasen NC, O'Leary DS, Flaum M, Nopoulos P, Watkins GL, Boles-Ponto LL, Hichwa RD (1997) Hypofrontality in schizophrenia: distributed dysfunctional circuits in neuroleptic-naive patients. Lancet 349:1730–1734.

Atchley WR, Rutledge JJ, Cowley ET (1981) Genetic components of size and shape. II. Multivaiate covariance patterns in the rat and mouse skull. Evolution 35:1037–1055.

Barta PE, Pearlson GD, Powers RE, Richards SS, Tune LE (1990) Auditory hallucinations and smaller superior temporal gyral volume in schizophrenia. Am J Psychiat 147:1457–1462.

Ben-Ari Y, Khazipov R, Leinekugel X, Caillard O, Gaiarsa JL (1997)

GABAA, NMDA and AMPA receptors: a developmentally regulated 'menage a trois'. Trends Neurosci 20:523–529.
Benes FM, Khan Y, Vincent SL, Wickramasinghe R (1996) Differences in the subregional and cellular distribution of GABA-A receptor binding in the hippocampal formation of schizophrenic brain. Synapse 22:338–349.
Beran R, Srivastava MS (1985) Bootstrap tests and confidence regions for functions of a covariance matrix. Ann Statist 13:95–115.
Berman KF, Torrey EF, Daniel DG, Weinberger DR (1992) Regional cerebral blood flow in monozygotic twins discordant and concordant for schizophrenia. Arch Gen Psychiat 49:927–934.
Berry M, Standring, S.M., Bannister, L.H. (1995) Nervous system. In: Gray's anatomy (Williams PL, Bannister LH, Berry MH, Collins P, Dyson M, Dussek JE, Ferguson MWJ, eds). Edinburgh: Churchill Livingstone.
Bertolino A, Saunders RC, Mattay VS, Bachevalier J, Frank JA, Weinberger DR (1997) Altered development of prefrontal neurons in rhesus monkeys with neonatal mesial temporo-limbic lesions: a proton magnetic resonance spectroscopic imaging study. Cereb Cortex 7:740–748.
Bertolino A, Callicot JH, Elman I, Mattay VS, Tedeschi G, Frank JA, Breier A, Weinberger DR (1998) Regionally specific neuronal pathology in untreated patients with schizophrenia: a proton magnetic resonance spectroscopic imaging study. Biol Psychiat 43:641–648.
Bogerts B, Lieberman JA, Ashtari M, Bilder RM, Degreef G, Lerner G, Johns C, Masiar S (1993) Hippocampus-amygdala volumes and psychopathology in chronic schizophrenia. Biol Psychiat 33:236–246.
Bookstein FL (1991) Morphometric tools for landmark data. Cambridge: Cambridge University Press.
Breier A, Buchanan RW, Elkashef A, Munson RC, Kirkpatrick B, Gellad F (1992) Brain morphology and schizophrenia. A magnetic resonance imaging study of limbic, prefrontal cortex, and caudate structures. Arch Gen Psychiat 49:921–926.
Brodmann K (1909) Vergleichende Lokalisationslehre der Grosshirnrinde. Leipzig: Barth.
Buchanan PK, Vladar K, Barta PE, Pearlson GD (1998) Structural evaluation of the prefrontal cortex in schizophrenia. Am J Psychiat 155:1049–1055.
Bullmore E, Brammer M, Rouleau G, Everitt B, Simmons A, Sharma T, Frangou S, Murray R, Dunn G (1995) Computerized brain tissue classification of magnetic resonance images: a new approach to the problem of partial volume artifact. NeuroImage 2:133–147.
Bullmore ET, Rabe-Hesketh S, Morris RG, Williams SCR, Gregory L, Gray JA, Brammer MJ (1996) Functional magnetic resonance image analysis of a large-scale neuro-cognitive network. NeuroImage 4:6–33.
Bullmore ET, Woodruff PWR, Wright IC, Rabe-Hesketh S, Howard RJ, Shuriquie N, Murray RM (1998) Does dysplasia cause anatomical dysconnectivity in schizophrenia? Schizophr Res 30:127–135.
Cannon TD, Mednick SA, Parnas J (1989) Genetic and perinatal determinants of structural brain deficits in schizophrenia. Arch Gen Psychiat 46:883–889.
Cheverud JM (1982) Phenotypic, genetic, and environmental morphological integration in the cranium. Evolution 36:499–516.
Cheverud JM (1984) Quantitative genetics and developmental constraints on evolution by selection. J Theor Biol 110:155–171.
Coull JT, Frith CD, Frackowiak RSJ, Grasby PM (1996) A fronto-parietal network for rapid visual information processing: a PET study of sustained attention and working memory. Neuropsychologia 34:1085–1095.
Csernansky JG, Joshi S, Haller JH, Gado M, Miller JP, Grenander, Miller MI (1998) Hippocampal morphometry in schizophrenia by high dimensional brain mapping. Proc Natl Acad Sci USA 95:11406–11411.
Curtis V, Bullmore ET, Brammer MJ, Wright IC, Williams SCR, Morris RG, Sharma TS, Murray RM, McGuire PK (1998) Attenuated frontal activation during verbal fluency in patients with schizophrenia. Am J Psychiat 155:1056–1063.
Daviss SR, Lewis DA (1995) Local circuit neurons of the prefrontal cortex in schizophrenia: selective increase in the density of calbindin-immunoreactive neurons. Psychiat Res 59:81–96.
Degreef G, Ashtari M, Bogerts B, Bilder RM, Jody DN, Alvir JM, Lieberman JA (1992) Volumes of ventricular system subdivisions measured from magnetic resonance images in first-episode schizophrenic patients. Arch Gen Psychiat 49:531–537.
DeLisi LE, Hoff AL, Schwartz JE, Shields GW, Halthore SN, Gupta SM, Henn FA, Anand AK (1991) Brain morphology in first-episode schizophrenic-like psychotic patients: a quantitative magnetic resonance imaging study. Biol Psychiat 29:159–175.
Dempsey PJ, Townsend GC, Martin NG, Neale MC (1995) Genetic covariance structure of incisor crown size in twins. J Denr Res 74:1389–1398.
Efron B, Tibshirani, R.J. (1993) An introduction to the bootstrap. New York: Chapman and Hall.
Falkai P, Bogerts B (1986) Cell loss in the hippocampus of schizophrenics. Eur Arch Psychiat Neurol Sci 236:154–161.
Flaum M, Swayze VW, II, DS OL, Yuh WT, Ehrhardt JC, Arndt SV, Andreasen NC (1995) Effects of diagnosis, laterality, and gender on brain morphology in schizophrenia. Am J Psychiat 152:704–714.
Frangou S, Sharma, T., Sigmundsson, T., Barta, P., Pearlson, G., Murray, R.M. (1997) The Maudsley Family Study. 4. Normal planum temporale asymmetry in familial schizophrenia. A volumetric MRI study. Br J Psychiat 170:328–333.
Friston KJ, Frith C (1995) Schizophrenia: a disconnection syndrome? Clin Neurosci 3:89–97.
Friston KJ, Frith CD, Liddle PF, Frackowiak RSJ (1993) Functional connectivity: the principal-component analysis of large (PET) data sets. J Cereb Blood Flow Metab 13:5–14.
Friston KJ, Herold S, Fletcher P, Silbersweig D, Cahill C, Dolan RJ, Liddle PF, Frackowiak RSJ, Frith CD (1994) Abnormal fronto-temporal interactions in schizophrenia. In: Biology of scizophrenia and affective disease (Watson SJ, ed.). ARNMD Series.
Friston KJ, Holmes AP, Worsley KJ (1995) Statistical parametric maps in functional imaging: a general approach. Hum Brain Map 2:189–210.
Glantz LA, Lewis DA (1997) Reduction of synaptophysin immunoreactivity in the prefrontal cortex of subjects with schizophrenia. Regional and diagnostic specificity. Arch Gen Psychiat 54:943–952.
Goldman-Rakic PS (1988) Topography of cognition: parallel distributed networks in primate association cortex. Annu Rev Neurosci 11:137–156.
Goldman-Rakic PS, Selemon LD (1997) Functional and anatomical aspects of prefrontal pathology in schizophrenia. Schizophr Bull 23:437–458.
Harris EF, Smith RJ (1982) Occlusion and arch size in families: a principal components analysis. Angle Orthodont 52:135–143.
Harvey I, Ron MA, Du Boulay G, Wicks D, Lewis SW, Murray RM (1993) Reduction of cortical volume in schizophrenia on magnetic resonance imaging. Psychol Med 23:591–604.
Jeste DV, Lohr JB (1989) Hippocampal pathologic findings in schizophrenia: a morphometric study. Arch Gen Psychiat 46:1019–1024.
Johnston MC, Bronsky PT (1995) Prenatal craniofacial development: new insights on normal and abnormal mechanisms. Crit Rev Oral Biol Med 6:368–422.
Joliffe IT (1986) Principal components analysis. New York: Springer-Verlag.
Kawasaki Y, Maeda Y, Urata K, Higashima M, Yamaguchi N, Suzuki M, Takashima T, Ide Y (1993) A quantitative magnetic resonance imaging study of patients with schizophrenia. Eur Arch Psychiat Clin Neurosci 242:268–272.
Kerwin RW (1993) Glutamate receptors, microtubule associated proteins and developmental anomaly in schizophrenia: an hypothesis. Psychol Med 22:547–551.
Kolb B, Sutherland RJ, Whishaw IQ (1983) Abnormalities in cortical and subcortical morphology after neonatal neocortical lesions in rats. Exp Neurol 79:223–244.
Kolb B, Cioe J, Muirhead D (1998) Cerebral morphology and functional sparing after prenatal frontal cortex lesions in rats. Behav Brain Res 91:143–155.
Kovelman JA, Scheibel AB (1984) A neurohistologic correlate of schizophrenia. Biol Psychiat 19:1601–21.
Krzanowski WJ (1979) Between-groups comparison of principal components. J Am Statist Assoc 74:703–707.
Krzanowski WJ (1988) Principles of multivariate analysis: a user's perspective. Oxford: Oxford University Press.
Lane A, Kinsella A, Murphy P, Byrne M, Keenan J, Colgan K, Cassidy B, Sheppard N, Horgan R, Waddington JL, Larkin C, O'Callaghan E (1997) The anthropometric assessment of dysmorphic features in schizophrenia as an index of its developmental origins. Psychol Med 27:1155–1164.
Lange N, Ryan L (1989) Assessing normality in random effects models. Ann Statist 17:624–642.
Lawrie SM, Abukmeil SS (1998) Brain abnormality in schizophrenia. A

systematic and quantitative review of volumetric magnetic resonance imaging studies. Br J Psychiat 172:110–120.

Lewis DA (1997) Schizophrenia and disordered neural circuitry. Schizophr Bull 23:529–531.

Lim KO, Sullivan EV, Zipursky RB, Pfefferbaum A (1996) Cortical gray matter volume deficits in schizophrenia: a replication. Schizophr Res 20:157–164.

Lofsvold D (1986) Quantitative genetics of morphological differentiation in Peromyscus. I. Tests of the homogeneity of geneic covariance structure among species and subspecies. Evolution 40:559–573.

Mai JK, Assheuer J, Paxinos G (1997) Atlas of the human brain. San Diego, CA: Academic Press.

McCarthy G, Luby M, Gore J, Goldman-Rakic P (1997) Infrequent events transiently activate human prefrontal and parietal cortex as measured by functional MRI. J Neurophysiol 77:1630–1634.

McGuire PK, Frith CD (1996) Disordered functional connectivity in schizophrenia. Psychol Med 26:663–667.

McGuire PK, Shah, G.M., Murray, R.M. (1993) Increased blood flow in Broca's area during auditory hallucinations in schizophrenia. Lancet 342:703–706.

McIntosh A, Grady C, Ungerleider L, Haxby J, Rapoport S, Horwitz B (1994) Network analysis of cortical visual pathways mapped with PET. J Neurosci 14:655–666.

Mellers JD, Bullmore E, Brammer M, Williams SC, Andrew C, Sachs N, Andrews C, Cox TS, Simmons A, Woodruff P (1995) Neural correlates of working memory in a visual letter monitoring task: an fMRI study. NeuroReport 7:109–112.

Mesulam M-M (1985) Principles of behavioral neurology. Philadelphia: Davis.

Moscovitch C, Kapur S, Kohler S, Houle S (1995) Distinct neural correlates of visual long-term memory for spatial location and object identity: a positron emission tomography study in humans. Proc Natl Acad Sci USA 92:3721–3725.

Mossey PA, McColl JH, Stirrups DR (1997) Differentiation between cleft lip with or without cleft palate and isolated cleft palate using parental cephalometric parameters. Cleft Palate Craniofac J 34:27–35.

Murray RM, Lewis SW (1987) Is schizophrenia a neurodevelopmental disorder? Br Med J Clin Res Ed 295:681–682.

Nelson MD, Saykin AJ, Flashman LA, Riordan HJ (1998) Hippocampal volume reduction in schizophrenia as assessed by magnetic resonance imaging. Arch Gen Psychiat 55:433–440.

Olson E, Miller, R. (1958) Morphological integration. Chicago, IL: University of Chicago Press.

Pandya DN, Yeterian EH (1985) Architecture and connections of cortical association areas. In: Cerebral cortex (Peters A, Jones EG, eds). New York: Plenum Press.

Paulsen SM (1994) Quantitative genetics of butterfly wing color patterns. Devel Genet 15:79–81.

Paxinos G (1990) The human nervous system. San Diego, CA: Academic Press.

Perneger TV (1998) What's wrong with Bonferroni adjustments. Br Med J 316:1236–1238.

Petrides M, Pandya DN (1988) Association fiber pathways to the frontal cortex from the superior temporal region in the rhesus monkey. J Comp Neurol 273:52–66.

Rajkowska G, Goldman-Rakic PS (1995) Cytoarchitectonic definition of prefrontal areas in the normal human cortex: II. Variability in locations of areas 9 and 46 and relationship to the Talairach coordinate system. Cereb Cortex 5:323–337.

Rajkowska G, Selemon LD, Goldman-Rakic PS (1998) Neuronal and glial somal size in the prefrontal cortex. Arch Gen Psychiat 55:2150–2224.

Robb RA (ed.) (1990) A software system for interactive and quantitative analysis of biomedical images. 3D Imaging in Medicine, NATO ASI Series, Vol. F60.

Ross CA, Pearlson GD (1996) Schizophrenia, the heteromodal association neocortex and development: potential for a neurogenetic approach. Trends Neurosci 19:171–176.

Saksena SS, Bixler D (1990) Facial morphometrics in the identification of gene carriers of X-linked hypohidrotic ectodermal dysplasia. Am J Med Genet 35:105–114.

Salmon E, Van der Linden M, Collette F, Delfiore G, Maquet P, Degueldre C, Luxen A, Franck G (1996) Regional brain activity during working memory tasks. Brain 119:1617–1625.

Saunders RC, Kolochana BS, Bachevalier J, Weinberger DR (1998) Neonatal lesions of the medial temporal lobe disrupt prefrontal cortical regulation of striatal dopamine. Nature 393:169–171.

Schlaepfer TE, Harris GJ, Tien AY, Peng LW, Lee S, Federman EB, Chase GA, Barta PE, Pearlson GD (1994) Decreased regional cortical gray matter volume in schizophrenia. Am J Psychiat 151:842–848.

Selemon LD, Rajkowska G, Goldman Rakic PS (1995) Abnormally high neuronal density in the schizophrenic cortex. A morphometric analysis of prefrontal area 9 and occipital area 17. Arch Gen Psychiat 52:805–818.

Selemon LD, Rajkowska G, Goldman Rakic PS (1998) Elevated neuronal density in prefrontal area 46 in brains from schizophrenic patients: application of a three-dimensional, stereologic counting method. J Comp Neurol 392:402–412.

Seow WK, Urban S, Vafaie N, Shusterman S (1998) Morphometric analysis of the primary and permanent dentitions in hemifacial microsomia: a controlled study. J Dent Res 77:27–38.

Sharma T, Lancaster E, Lee D, Lewis S, Sigmundsson T, Takei N, Gurling H, Barta P, Pearlson G, Murray R (1998) The Maudsley Study V: brain changes in familial schizophrenics and their relatives: a volumetric MRI study. Br J Psychiat 173:132–138.

Shenton ME, Kikinis R, Jolesz FA, Pollak SD, LeMay M, Wible CG, Hokama H, Martin J, Metcalf D, Coleman M, *et al.* (1992) Abnormalities of the left temporal lobe and thought disorder in schizophrenia. A quantitative magnetic resonance imaging study. N Engl J Med 327:604–612.

Suddath RL, Christison GW, Torrey EF, Casanova MF, Weinberger DR (1990) Anatomical abnormalities in the brains of monozygotic twins discordant for schizophrenia. N Engl J Med 322:789–794.

Sullivan EV, Lim KO, Mathalon D, Marsh L, Beal DM, Harris D, Hoff AL, Faustman WO, Pfefferbaum A (1998) A profile of cortical gray matter volume deficits characteristic of schizophrenia. Cereb Cortex 8:117–124.

Suzuki M, Yuasa S, Minabe Y, Murata M, Kurachi M (1993) Left superior temporal blood flow increases in schizophrenic and schizophreniform patients with auditory hallucination: a longitudinal case study using ^{123}I-IMP SPECT. Eur Arch Psychiat Clin Neurosci 242:257–261.

Talairach J, Tournoux P (1988) Co-planar stereotaxic atlas of the human brain. Stuttgart: Thieme Verlag.

Tien AY, Eaton WW, Schlaepfer TE, McGilchrist IK, Menon R, Powers R, Aylward E, Barta P, Strauss ME, Pearlson GD (1996) Exploratory factor analysis of MRI brain structure measures in schizophrenia. Schizophr Res 19:93–101.

Van Essen DC (1997) A tension-based theory of morphogenesis and compact wiring in the central nervous system. Nature 385:313–318.

Van Horn JD, McManus IC (1992) Ventricular enlargement in schizophrenia. A meta-analysis of studies of the ventricle:brain ratio (VBR). Br J Psychiat 160:687–697.

Vitt LJ, Caldwell JP, Zani PA, Titus TA (1997) The role of habitat shift in the evolution of lizard morphology: evidence from tropical Tropidurus. Proc Natl Acad Sci USA 94:3828–3832.

Ward KE, Friedman L, Wise A, Schulz SC (1996) Meta-analysis of brain and cranial size in schizophrenia. Schizophr Res 22:197–213.

Weickert CS and Weinberger DR (1998) A candidate molecule approach to defining developmental pathology in schizophrenia. Schizophr Bull 24:303–316.

Weinberger DR (1987) Implications of normal brain development for the pathogenesis of schizophrenia. Arch Gen Psychiat 44:660–669.

Weinberger DR (1996) Schizophrenia as a developmental disorder. In: Schizophrenia Hirsch SR, Weinberger DR, eds). Oxford: Blackwell Science.

Weinberger DR, Berman KF, Suddath R, Torrey EF (1992) Evidence of dysfunction of a prefrontal–limbic network in schizophrenia: a magnetic resonance imaging and regional cerebral blood flow study of discordant monozygotic twins. Am J Psychiat 149: 890–897.

Wernicke C (1894) Grundriss der Psychiatrie in Kliniscen Vorlesungen. Leipzig: Verlag von Georg Thieme.

Woo TU, Whitehead RE, Melchitzky DS, Lewis DA (1998) A subclass of prefrontal gamma-aminobutyric acid axon terminals are selectively altered in schizophrenia. Proc Natl Acad Sci USA 95:5341–5346.

Woodruff P, Brammer M, Mellers J, Wright I, Bullmore E, Williams S (1995) Auditory hallucinations and perception of external speech. Lancet 346:1035.

Woodruff PW, Wright IC, Bullmore ET, Brammer M, Howard RJ, Williams

SC, Shapleske J, Rossell S, David AS, McGuire PK, Murray RM (1997) Auditory hallucinations and the temporal cortical response to speech in schizophrenia: a functional magnetic resonance imaging study. Am J Psychiat 154:1676–1682.

Wright IC, McGuire PK, Poline J-B, Travere JM, Murray RM, Frith CD, Frackowiak RSJ, Friston KJ (1995) A voxel-based method for the statistical analysis of grey and white matter applied to schizophrenia. NeuroImage 2:244–252.

Wright IC, Ellison ZR, Sharma T, Friston KJ, Murray R, McGuire PK (1999) Mapping of gray matter changes in schizophrenia. Schizophr Res 35:1–14.

Young CE, Arima K, Xie J, Hu L, Beach TG, Falkai P, Honer WG (1998) SNAP-25 deficit and hippocampal connectivity in schizophrenia. Cereb Cortex 8:261–268.

Young MP (1993) The organization of neural systems in the primate cerebral cortex. Proc R Soc Lond B Biol Sci 252:13–18.

Zipursky RB, Lim KO, Sullivan EV, Brown BW, Pfefferbaum A (1992) Widespread cerebral gray matter volume deficits in schizophrenia. Arch Gen Psychiat 49:195–205.

Zipursky RB, Lambe EK, Kapur S, Mikulis DJ (1998) Cerebral gray matter volume deficits in first episode psychosis. Arch Gen Psychiat 55:540–546.

Appendix 1

Coordinates of cerebral and ventricular regions

Brodmann no.	Coordinates
1, 2, 3	65 –8 24, 60 –15 28, 65 –10 32, 30 –22 35, 40 –15 35, 55 –10 35, 60 –18 35, 60 –25 40, 35 –23 40, 50 –20 45, 40 –20 45, 45 –20 50, 50 –22 55, 40 –30 60, 35 –30 65
4	60 –5 16, 60 2 20, 65 2 24, 60 –3 32, 25 –15 35, 35 –10 35, 54 –5 35, 45 –15 40, 60 –11 40, 25 –16 40, 55 –5 45, 40 –15 45, 30 –15 45, 30 –20 50, 35 –10 50, 50 –5 50, 42 –7 55, 35 –20 55, 15 –25 55, 45 –15 60, 25 –25 60, 15 –30 60, 35 –22 65, 25 –22 65, 10 –30 65
5	5 –35 50, 4 –45 60, 40 –40 60, 10 –38 65, 25 –38 65, 36 –38 65
6	60 5 8, 60 5 12, 50 0 12, 60 5 16, 60 8 20, 60 10 24, 60 –5 28, 50 –2 28, 60 5 32, 40 5 35, 60 2 35, 60 –5 40, 42 –4 40, 25 –10 40, 5 20 45, 27 10 45, 52 8 45, 30 0 50, 45 15 50, 45 8 50, 5 10 50, 5 –5 50, 5 –15 50, 5 15 55, 5 0 55, 5 –15 55, 40 10 55, 25 20 55, 8 –22 55, 25 –13 55, 33 –3 55, 47 0 55, 20 10 60, 40 –5 60, 5 –15 60, 25 –15 60, 15 –10 65, 5 –15 65, 30 –15 65, 33 –20 65, 27 –20 65, 18 –19 65, 5 –24 65
7	5 –55 32, 10 –60 35, 10 –70 35, 10 –50 40, 10 –70 40, 5 –40 45, 5 –50 45, 5 –70 45, 15 –75 45, 35 –70 45, 5 –45 50, 5 –55 50, 10 –65 50, 25 –65 50, 40 –60 50, 5 –35 55, 5 –55 55, 15 –65 55, 40 –55 55, 20 –50 60, 40 –40 60, 5 –55 60, 25 –30 60, 25 –45 65, 10 –41 65, 36 –41 65
8	10 45 40, 25 45 40, 40 35 40, 10 35 40, 10 35 45, 15 30 45, 35 30 45, 45 20 45, 5 40 50, 5 25 50, 20 40 50, 35 35 50, 40 25 50, 5 30 55, 20 30 55
9	5 50 16, 5 45 20, 5 55 24, 5 45 24, 40 50 24, 10 60 28, 25 55 28, 25 50 28, 5 45 28, 55 25 28, 40 23 28, 20 55 32, 5 50 32, 40 35 32, 15 53 35, 10 36 35, 37 37 35, 52 18 35, 60 10 40, 50 25 40, 38 11 40
10	40 60 –8, 5 48 –8, 5 65 –4, 35 60 –4, 5 60 –1, 25 60 –1, 45 50 –1, 5 60 4, 35 60 4, 5 60 8, 20 70 8, 35 60 8, 20 65 12, 40 55 12, 5 55 12, 5 60 16, 35 60 16, 5 60 20, 20 60 20, 40 50 20, 15 60 24
11	10 45 –28, 10 40 –24, 3 25 –24, 10 20 –20, 15 30 –20, 5 30 –16, 30 30 –16, 33 55 –12, 5 33 –12
12	60 3 –8
17	10 –95 –12, 3 –90 –8, 20 –100 –8, 5 –85 –4, 5 –100 –1, 10 –95 4, 5 –80 8, 5 –80 12
18	25 –95 –12, 20 –75 –8, 30 –90 –8, 5 –80 –4, 10 –100 –4, 30 –95 –4, 10 –70 –1, 5 –85 –1, 30 –95 –1, 10 –55 4, 10 –80 4, 30 –95 4, 25 –95 8, 5 –90 12, 12 –100 12, 35 –90 12, 15 –95 16, 5 –85 16, 10 –85 20, 20 –90 20, 5 –80 24, 5 –70 28
19	50 –70 –12, 40 –85 –12, 20 –60 –8, 45 –80 –8, 25 –45 –4, 20 –70 –4, 15 –55 –1, 50 –70 –1, 45 –80 4, 50 –80 8, 40 –85 8, 50 –80 12, 45 –85 16, 25 –95 16, 35 –85 20, 45 –82 20, 10 –90 24, 35 –85 24, 45 –80 28, 25 –85 28, 10 –85 28, 5 –90 32, 20 –85 32, 45 –75 32, 10 –80 35, 33 –80 35, 55 –70 35, 10 –80 40, 25 –75 40, 40 –70 40
20	30 –5 –40, 30 –5 –36, 33 –10 –32, 25 –10 –28, 45 –15 –28, 50 –22 –24, 60 –8 –20, 60 –25 –20, 20 –25 –16, 60 –40 –16, 33 –42 –16, 5 15 –4
21	15 7 –28, 55 3 –24, 55 5 –20, 60 5 –16, 60 –10 –16, 60 3 –12, 60 –22 –12, 60 –3 –8, 60 –20 –8, 60 –40 –8, 60 –5 –4, 60 –30 –4, 65 –5 –1, 50 –40 –1, 65 –20 –1, 65 –40 –1, 60 –45 4, 60 –45 8
22	50 10 –4, 55 7 –1, 55 0 4, 60 –30 4, 60 –35 8, 60 –40 12, 35 –45 12, 65 –35 16, 60 –55 16, 36 –40 16, 60 –50 20, 60 –40 20
23	5 –55 8, 5 –60 12, 5 –55 16, 10 –60 20, 5 –27 24, 5 –42 24, 10 –30 28, 10 –15 28, 5 –20 32
24	5 30 –4, 5 35 –1, 5 28 4, 5 29 8, 5 26 12, 5 22 16, 5 15 20, 5 5 24, 10 –5 28, 10 15 28, 5 5 32, 10 5 35, 10 –15 35, 10 0 40, 10 –15 40, 5 –5 45
25	5 20 –16, 10 10 –16, 5 20 –12, 10 5 –12, 3 10 –8
27	–25 –30 –4, 15 –30 –1
28	50 2 –28, 16 3 –24, 25 10 –20, 22 –15 –20, 30 10 –16, 20 –15 –16, –20 –15 –12, 20 –30 –8
29	10 –40 8, 5 –38 12, 10 –40 20
30	15 –40 –4, 18 –40 –1, 5 –50 8, 5 –50 12, 5 –40 16, 10 –50 20
31	5 –65 8, 5 –65 12, 5 –60 16, 10 –65 20, 5 –55 24, 10 –55 28, 10 –40 28, 10 –55 28, 10 –40 28, 5 –40 32, 10 –35 35, 10 –48 35, 10 –25 40, 10 –45 40
32	3 40 –8, 3 25 –8, 5 40 –4, 5 45 –1, 5 45 4, 5 45 8, 5 40 12, 5 40 16, 5 35 20, 5 33 24, 10 30 28, 5 25 32, 8 20 35, 10 25 40, 10 10 40, 5 5 45
34	12 –2 –20, 15 2 –16, 20 2 –12
35	20 –12 –24, 35 –25 –16, 20 –25 –12, 20 –35 –8
36	25 –22 –24, 30 –25 –20, 40 –35 –20, 25 –35 –16, 25 –40 –12, 20 –40 –8
37	40 –50 –16, 50 –60 –16, 60 –45 –12, 35 –50 –12, 55 –60 –12, 20 –50 –8, 60 –50 –8, 55 –70 –8, 55 –60 –4, 60 –60 –1, 50 –55 –1, 60 –60 4, 60 –63 4, 55 –70 4, 45 –60 4, 60 –60 8
38	30 5 –40, 30 5 –36, 33 10 –32, 40 20 –28, 30 15 –24, 50 15 –20, 45 20 –16, 52 10 –12, 60 10 –8
39	60 –70 8, 60 –60 12, 55 –60 16, 50 –75 16, 60 –65 20, 52 –75 20, 60 –55 24, 45 –75 24, 60 –60 28, 50 –73 28, 55 –60 32, 60 –60 35
40	60 –20 16, 60 –25 20, 60 –40 24, 60 –20 24, 60 –25 28, 60 –40 28, 60 –20 32, 60 –40 32, 60 –30 35, 60 –45 35, 47 –32 35, 47 –43 35, 50 –65 40, 60 –45 40, 60 –35 40, 50 –55 45, 50 –40 45, 50 –30 45, 45 –50 50, 50 –40 50, 50 –30 50, 45 –45 55
41	40 –25 12, 30 –35 12
42	60 –10 8, 60 –25 8, 60 –10 12, 65 –25 16, 50 –30 20
43	60 –10 16, 65 –10 20
44	55 15 8, 60 23 12, 50 15 12, 55 15 16, 60 15 20, 50 20 24, 60 10 28, 47 8 28, 55 20 32
45	55 40 4, 55 30 4, 55 20 4, 40 32 4, 60 25 8, 45 28 8, 60 35 12, 44 30 12, 55 25 16, 50 25 20
46	45 50 4, 30 40 4, 50 50 8, 50 40 8, 45 45 12, 33 36 12, 45 50 16, 50 37 16, 47 35 20, 50 30 24, 33 30 24, 45 40 24, 45 42 28
47	15 25 –24, 25 20 –20, 30 20 –16, 45 45 –12, 45 28 –12, 50 15 –12, 40 18 –12, 50 45 –8, 48 25 –8, 50 18 –8, 40 50 –4, 60 30 –4, 50 30 –1, 33 33 –1
Hippocampus	25 –5 –20, 30 –10 –16, 30 –10 –12, 30 –30 –8, 35 –30 –4, 35 –40 –1, 30 –40 4
Thalamus	5 –10 4, 15 –25 4, 15 –15 8, 10 –10 12, 15 –32 12, 5 –5 16, 20 –25 16
Corpus striatum	20 10 –8, 5 10 –4, 10 15 –1, 10 15 4, 10 15 8, 10 10 12, 15 15 16, 10 –5 16, 15 3 20, 20 –30 20, 15 –10 24
Putamen	20 0 –1, 20 0 4, 20 –15 4, 25 0 8, 20 5 12, 20 –10 12
Brain-stem	0 –40 –40, 0 –30 –36, 0 –35 –32, 0 –30 –28, 0 –30 –24, 0 –25 –20, 0 –30 –16, 0 –30 –12, 0 –15 –8, 0 –33 –8, 0 –15 –4, 0 –30 –4, 0 –10 –1, 0 –30 –1
Cerebellum	18 –50 –40, 40 –70 –40, 0 –55 –36, 30 –55 –36, 0 –60 –32, 30 –50 –32, 0 –60 –28, 25 –50 –28, 0 –60 –24, 30 –40 –24, 0 –45 –20, 25 –35 –20, 35 –42 –20, 0 –50 –16, 20 –33 –16, 23 –40 –16, 25 –50 –16, 33 –55 –16, 40 –75 –16, 15 –38 –12, 20 –45 –12, 30 –55 –12, 25 –73 –12, 0 –50 –12, 0 –73 –12, 5 –45 –8, 15 –45 –8, 15 –60 –8, 0 –55 –4, 10 –40 –4, 10 –65 –4, 0 –55 –1
Insula	50 15 –12, 35 10 –8, 40 25 –4, 40 –10 –4, 35 20 –1, 40 5 –1, 40 –10 –1, 30 25 4, 40 10 4, 40 –15 4, 35 22 8, 45 5 8, 40 –17 8, 35 25 12, 40 5 12, 40 –10 12, 35 –5 16, 34 –22 16, 32 –21 20

Appendix 1 – *continued*

Brodmann no.	Coordinates
Extra-cerebral	0 10 –40, 0 30 –40, 0 50 –40, 25 35 –40, 0 10 –36, 0 30 –36, 0 50 –36, 25 35 –36, 0 10 –32, 0 30 –32, 0 50 –32, 25 35 –32
Ventricles	
Frontal horn	10 24 12
Central	10 –15 20
Trigone	22 –35 12
Occipital horn	28 –60 12
Post. temp.	30 –35 –1
Temp. horn	30 –10 –20

Appendix 2
Principal components analysis

Brodmann no.	Region	PC1		PC2		PC3		PC4		PC5	
		Left	Right	Left	Right	Left	Right	Left	Right	Left	Right
	Frontal grey matter										
4	Precentral gyrus (M1)	0.12	0.12	0.06	0.02	0.01	–0.01	0.00	–0.01	–0.05	0.08
6	Premotor gyrus	0.12	0.12	0.03	0.02	0.10	0.12	0.01	–0.03	0.02	0.05
8	Dorsolateral prefrontal	0.10	0.10	0.02	0.02	0.17	0.18	–0.04	–0.08	0.11	0.10
9	Dorsolateral prefrontal	0.11	0.11	0.04	0.02	0.12	0.14	0.00	–0.09	0.13	0.17
10	Frontal pole	0.08	0.07	0.00	0.01	0.08	0.07	–0.18	–0.26	0.20	0.20
11	Orbitofrontal	0.07	0.07	–0.01	–0.03	0.15	0.17	–0.06	–0.13	0.11	0.15
12	Orbitofrontal	0.09	0.10	0.10	0.06	–0.04	0.02	0.08	–0.03	–0.02	0.03
32	Medial frontal	0.12	0.11	0.04	0.03	0.15	0.15	–0.05	–0.06	0.07	0.14
44	Inferior frontal	0.11	0.11	0.08	0.04	0.03	0.07	0.11	0.09	0.06	0.12
45	Inferior frontal	0.11	0.11	0.11	0.06	0.06	0.08	0.09	–0.03	0.02	0.03
46	Dorsolateral prefrontal	0.11	0.11	0.05	0.06	0.07	0.08	0.05	–0.14	0.09	0.14
47	Ventrolateral prefrontal	0.11	0.12	0.05	0.04	0.07	0.07	0.09	–0.02	–0.01	0.08
	Insula grey matter										
–	Insula	0.12	0.12	0.04	0.03	–0.01	–0.01	0.14	0.08	–0.02	0.08
	Temporal grey matter										
20	Inferior temporal gyrus	0.07	0.05	–0.04	0.01	0.00	–0.01	0.11	0.14	0.00	0.05
21	Middle temporal gyrus	0.12	0.12	0.04	0.03	0.01	0.01	0.07	0.08	–0.09	–0.05
22	Superior temporal gyrus	0.11	0.12	0.00	0.00	0.01	0.00	0.11	0.07	–0.13	–0.07
34	Uncus	0.09	0.07	–0.13	–0.16	0.12	0.10	–0.01	–0.05	–0.11	–0.10
–	Hippocampus	0.11	0.10	0.06	0.07	–0.01	0.04	0.10	0.13	–0.03	0.11
27	Subicular region	0.09	0.07	0.09	0.13	–0.23	–0.25	–0.10	–0.06	0.03	0.00
28	Parahippocampal region	0.11	0.11	0.04	0.03	–0.01	–0.01	0.11	0.10	–0.07	–0.02
35	Parahippocampal region	0.11	0.10	0.04	0.07	–0.02	–0.01	0.10	0.11	–0.05	0.06
36	Medial temporal	0.07	0.05	–0.09	0.04	0.04	0.00	0.08	0.10	–0.09	0.06
37	Inf-Post Temporal	0.11	0.11	0.00	0.05	–0.04	–0.04	–0.01	–0.04	–0.18	–0.08
38	Temporal pole	0.10	0.11	0.08	0.11	0.03	0.03	0.01	0.08	–0.02	0.12
41	Medial transverse temporal region (A1)	0.11	0.10	–0.02	–0.01	–0.02	–0.04	0.16	0.14	–0.11	–0.08
42	Lateral transverse temporal region	0.10	0.11	0.01	0.00	0.05	0.00	0.11	0.11	–0.13	–0.07
	Parietal grey matter										
1, 2, 3	Postcentral gyrus (S1)	0.12	0.12	0.05	0.03	0.00	–0.05	0.00	0.00	–0.05	0.03
5	Superior parietal lobule	0.10	0.09	0.02	0.03	0.10	0.09	–0.07	–0.09	–0.04	–0.13
7	Superior parietal lobule/precuneus	0.11	0.12	0.00	–0.02	0.13	0.10	–0.06	–0.09	–0.06	–0.08
39	Angular gyrus	0.12	0.12	0.01	0.03	0.05	0.01	0.00	0.03	–0.08	–0.09
40	Supramarginal gyrus	0.13	0.13	0.03	–0.01	0.02	0.00	0.03	0.01	–0.05	0.00
43	Inferior postcentral gyrus	0.10	0.10	0.09	0.00	–0.08	–0.05	0.02	0.06	–0.05	0.01
	Occipital grey matter										
17	Occipital (striate) (V1)	0.07	0.08	–0.07	–0.04	–0.03	–0.08	–0.28	–0.30	–0.22	–0.18
18	Occipital (parastriate)	0.10	0.11	–0.04	–0.01	–0.02	–0.06	–0.22	–0.21	–0.17	–0.11
19	Occipital (peristriate)	0.12	0.12	0.00	–0.01	0.02	–0.03	–0.12	–0.09	–0.10	–0.06
	Cingulate grey matter										
24	Anterior cingulate gyrus	0.12	0.11	–0.05	–0.06	0.07	0.09	0.08	0.04	0.01	0.04
25	Subcallosal	0.05	0.05	–0.15	–0.14	0.10	0.06	–0.17	–0.22	–0.08	–0.06
23	Posterior cingulate gyrus	0.09	0.10	–0.11	–0.14	–0.04	–0.10	0.01	–0.02	–0.07	–0.04
31	Posterior cingulate gyrus	0.12	0.12	–0.06	–0.08	0.03	0.03	0.02	0.02	–0.06	–0.07
29	Retrosplenial	0.10	0.08	0.04	0.09	–0.22	–0.25	–0.06	–0.06	0.04	–0.01
30	Retrosplenial	0.11	0.11	–0.03	–0.04	–0.13	–0.14	0.00	0.01	–0.06	–0.02

Appendix 2 – *continued*

Brodmann no.	Region	PC1		PC2		PC3		PC4		PC5	
		Left	Right	Left	Right	Left	Right	Left	Right	Left	Right
	Subcortical grey matter										
–	Corpus striatum	0.10	0.08	–0.01	–0.01	–0.08	–0.14	–0.06	–0.17	0.14	0.22
–	Putamen	0.09	0.07	0.05	0.04	–0.16	–0.19	0.02	–0.08	0.10	0.23
–	Thalamus	0.10	0.09	0.03	0.07	–0.22	–0.25	–0.03	–0.05	0.09	0.07
–	Brain Stem	0.10	0.10	0.04	0.04	–0.22	–0.22	–0.04	–0.03	0.07	0.07
–	Cerebellum	0.10	0.10	–0.05	–0.04	–0.03	0.00	–0.03	–0.02	–0.19	–0.16
	Ventricular										
–	Ventricular frontal pole	–0.06	–0.05	0.25	0.25	0.08	0.04	–0.02	–0.03	–0.10	–0.14
–	Ventricular central	–0.05	–0.04	0.28	0.28	0.07	0.05	–0.08	–0.07	–0.11	–0.15
–	Ventricular trigone	–0.05	–0.04	0.28	0.29	0.06	0.03	–0.05	–0.03	–0.02	–0.12
–	Ventricular occipital pole	–0.04	–0.04	0.24	0.26	0.04	–0.01	–0.05	–0.08	0.04	–0.08
–	Ventricular posterior temporal	–0.05	–0.05	0.24	0.23	0.07	0.05	–0.05	–0.01	0.02	–0.07
–	Ventricular anterior temporal horn	–0.05	–0.03	0.05	0.02	–0.01	0.02	–0.13	–0.18	–0.01	0.06
	75% confidence cone index d_k		0.99		0.88		0.71		0.43		0.28
	Similarity coefficient κ		0.92		0.74		0.62		0.50		0.47